



OPEN

## Ferulic acid derivatives block coronaviruses HCoV-229E and SARS-CoV-2 replication in vitro

Sébastien Pasquereau<sup>1,6</sup>, Mathilde Galais<sup>2,6</sup>, Maxime Bellefroid<sup>2,6</sup>, Irene Pachón Angona<sup>3</sup>, Stéphanie Morot-Bizot<sup>4</sup>, Lhassane Ismaili<sup>3</sup>, Carine Van Lint<sup>2,6</sup> & Georges Herbein<sup>1,5,6</sup>✉

A novel coronavirus, SARS-CoV-2, emerged in China at the end of 2019 causing a large global outbreak. As treatments are of the utmost importance, drugs with broad anti-coronavirus activity embody a rich and rapid drug discovery landscape, where candidate drug compounds could be identified and optimized. To this end, we tested ten small-molecules with chemical structures close to ferulic acid derivatives (FADs) (n = 8), caffeic acid derivatives (CAFDs) (n = 1) and carboxamide derivatives (CAMDs) (n = 1) for their ability to reduce HCoV-229E replication, another member of the coronavirus family. Among these ten drugs tested, five of them namely MBA112, MBA33, MBA27-1, OS4-1 and MBA108-1 were highly cytotoxic and did not warrant further testing. In contrast, we observed a moderate cytotoxicity for two of them, MBA152 and 5c. Three drugs, namely MBA140, LIJ2P40, and MBA28 showed lower cytotoxicity. These candidates were then tested for their antiviral properties against HCoV-229E and SARS-CoV2 replication. We first observed encouraging results in HCoV-229E. We then measured a reduction of the viral SARS-CoV2 replication by 46% with MBA28 (EC50 > 200 µM), by 58% with MBA140 (EC50 = 176 µM), and by 82% with LIJ2P40 (EC50 = 66.5 µM). Overall, the FAD LIJ2P40 showed a reduction of the viral titer on SARS-CoV-2 up to two logs with moderate cytotoxicity which opens the door to further evaluation to fight Covid-19.

Human coronaviruses (HCoV) are positive-stranded RNA pathogens that are known to be rapidly evolving viruses. The coronaviridae family encompasses six different strains infecting humans divided into two genera: alphacoronavirus (alphaCoV) and betacoronavirus (betaCoV)<sup>1</sup>. The low pathogenic HCoV-229E and HCoV-NL63 strains are part of the alphaCoV. The betaCoV genera ramifies into the A lineage strains, including the more pathogenic HCoV-OC43 and HCoV-HKU1, and into the B and C lineage, respectively including the highly pathogenic severe acute respiratory syndrome coronavirus (SARS-CoV) and SARS-CoV-2, and the Middle East respiratory syndrome coronavirus (MERS-CoV)<sup>2,3</sup>. The lower and moderately pathogenic strains are endemic in the human populations, where they account for 15–30% of mild, self-limiting respiratory infections. These strains, namely HCoV-229E, HCoV-NL63, HCoV-OC43, and HCoV-HKU1, still present a greater incidence of lower respiratory tract infection in immunocompromised individuals<sup>4</sup>. The highly pathogenic strains include both the 2002 SARS-CoV and the 2012 MERS-CoV, which are linked to acute respiratory distress syndrome (ARDS). This syndrome potentially engender a chronic reduction in lung function, arrhythmia, or death<sup>5</sup>, with a mortality rate of 9.6% for SARS-CoV and 35.5% for MERS-CoV. SARS-CoV-2, the etiological agent behind Covid-19 disease, emerged in December 2019 in the city of Wuhan in China. After its pandemic outbreak, it became a major public health concern, inducing worldwide emergency measures<sup>6</sup>. While the average symptoms of infection are mild compared to SARS-CoV and MERS-CoV, SARS-CoV-2 can result in severe symptoms including hyperinflammation, cytokine storm and multiple organ complications. It can ultimately lead to death for some individuals<sup>7</sup>.

Aside from fastly developed vaccines<sup>8</sup>, very few effective curative therapy is available against SARS-CoV-2. To date, the recently developed molnupinavir and the new combination of nirmatrelvir and ritonavir have shown the most promising effect on SARS-CoV-2. In addition to these drugs, the use of dexamethasone, tocilizumab

<sup>1</sup>Pathogens and Inflammation/EPILAB Laboratory, EA 4266, Université de Franche-Comté, Université Bourgogne Franche-Comté (UBFC), Besançon, France. <sup>2</sup>Service of Molecular Virology, Department of Molecular Biology (DBM), Université Libre de Bruxelles (ULB), 6041 Gosselies, Belgium. <sup>3</sup>Neurosciences Intégratives et Cliniques EA 481, Pôle de Chimie Organique et Thérapeutique, Univ. Bourgogne Franche-Comté, UFR Santé, Besançon, France. <sup>4</sup>Apex Biosolutions, Besançon, France. <sup>5</sup>Department of Virology, CHU Besançon, Besançon, France. <sup>6</sup>These authors contributed equally to this work: Sébastien Pasquereau, Mathilde Galais, Maxime Bellefroid, Carine Van Lint and Georges Herbein. ✉email: georges.herbein@univ-fcomte.fr

and baricitinib has been showed to improve the mortality in hospitalized patients with COVID-19<sup>9–12</sup>. Several drugs were previously used as curative therapies, but their efficiency were limited<sup>13</sup>. The development of new curative drugs is desperately needed<sup>14</sup>. It is well-known that it might take years for newly developed drugs to be clinically approved and reach the market<sup>15</sup>, despite the tremendous efforts put into their development. Repurposing existing drugs could be more effective than de novo drug discovery, with a reduced cost and time. A rapid evaluation of in vivo and in vitro efficacy is possible for existing drugs<sup>16</sup>. Additionally, drugs that were shown to inhibit the replication of other coronaviruses, including HCoV-229E, could potentially inhibit the replication of SARS-CoV-2 and other betacoronaviruses<sup>17</sup>.

Polyphenols have recently become an important group of compounds for the discovery of new drugs against human diseases<sup>18</sup>, including against Covid-19, as some recent studies already reported<sup>19</sup>. Recently we reported that resveratrol, a well-known nutraceutical with a multitude of biological properties and therapeutic applications belonging to polyphenols' stilbenoids group<sup>20</sup>, inhibits the replication of both HCoV-229E and SARS-CoV-2<sup>21</sup>. Resveratrol is known for its anti-inflammatory activity<sup>22</sup>, and for its anti-aging and antioxidant properties<sup>23</sup>. Resveratrol showed a potential as an anti-viral agent against some RNA and DNA viruses. Possible target RNA viruses include influenza virus<sup>24</sup>, Zika virus<sup>25</sup>, rhinovirus<sup>26</sup>, rotavirus<sup>27</sup> and MERS-CoV<sup>28</sup>, and DNA viruses including poxvirus<sup>29</sup> and polyomavirus<sup>30</sup>.

Therefore we decided to assess the anti-coronavirus activity of other phenolic compounds, namely ferulic acid derivatives (FADs) and one caffeic acid derivative (CAFD), in addition to a carboxamide derivative (CAMD). Phenolic compounds display antiviral activity against herpes simplex virus-1 and rabies virus<sup>31</sup>. Ferulic acid can be extracted from various fruits and cereals and is, with its derivatives, a phenolic compound. Ferulic acid derivatives have been shown to inhibit H1N1 influenza virus replication in vitro<sup>32</sup>. Caffeic acids are found in coffee, fruits, and vegetables, and constitute one of the abundant plant-based phenols, which structures include 2 phenolic hydroxyl moieties. Caffeic acid and its derivatives previously showed an antiviral activity against herpes simplex virus<sup>33</sup>, SFTS (severe fever with thrombocytopenia syndrome) virus<sup>34</sup>, and influenza virus<sup>35</sup>. In addition, like resveratrol, phenolic compounds including FADs and CAFDs exhibit potent antioxidant and anti-inflammatory properties<sup>36</sup>. Carboxamide derivatives have been shown to inhibit influenza virus, parainfluenza virus type 3, norovirus, SARS-CoV and recently SARS-CoV-2 replication in vitro<sup>37–41</sup>. Therefore we tested the anti-coronavirus activity of MBA140, a carboxamide derivative newly synthesized, which displays the closest chemical structure to an oxazole-carboxamide derivative previously reported as efficient against SARS-CoV<sup>41</sup>.

In the light of what was mentioned previously, we screened ten molecules with chemical structures close to already reported molecules with anti-SARS-CoV-2 protease activities<sup>42</sup> and belonging to the ferulic acid derivatives, caffeic acid derivatives, and carboxamide derivatives. For any of these drugs we tested in vitro the inhibitory effect on HCoV-229E and SARS-CoV2 replication.

## Materials and methods

**Viruses and reagents preparation.** HCoV-229E was isolated from nasal and throat swabs collected from a man with mild upper respiratory illness (Human Coronavirus 229E ATCC VR-740). HCoV-229E stock virus (5 log PFU/mL) was propagated using MRC5 cells (RD Biotech, Besançon, France). MRC5 cells were cultured in DMEM media supplemented with 10% FCS. The infectious clone SARS-CoV-2 mNeonGreen (icSARS-CoV-2-mNG) strain was provided by Dr. Pei Yong Shi from University of Texas Medical Branch (UTMB)<sup>43</sup>. SARS-CoV-2-mNG stock virus (7 log TCID<sub>50</sub>/mL) was propagated in Vero E6 cells (ATCC) in DMEM media supplemented with 2% FCS. Viral titers were determined by endpoint dilution assays on Vero E6 cells and stored at – 80 °C until use.

**Drug preparation.** The ten small molecules tested were synthesized at the University of Franche-Comté. As described previously<sup>44–47</sup>, the molecules were synthesized using the Ugi-4MCR method, starting from ferulic acid, caffeic acid or carboxamide. The resulting compounds were purified using flash column chromatography. After purification, drugs were stored in solid form at – 20 °C before preparation. Drugs were diluted in DMSO at a concentration of 10 mM, based on their molecular weight. The 10 mM stock was further diluted in cell culture media at final assay concentration at the time of use (1, 5, 10, 50, 100 or 200 μM).

**Viral replication assay.** MRC5 cells were infected with HCoV-229E at MOI=1 and treated at time of infection with compounds diluted in culture media during a 2-h incubation period. After removing the inoculum the cells were overlaid with culture media containing diluted compounds. Supernatants were collected after a 48-h incubation at 37 °C, to quantify viral loads by RT-qPCR and by plaque forming unit (PFU) assay as previously described<sup>21,48,49</sup>. For RT-qPCR, RNA was extracted using an RNA extraction kit (EZNA Total kit I, Omega BIO-TEK, Norcross, GA). RT-qPCR was performed based on a previously described protocol<sup>49</sup>, adapted using Superscript IV RT kit (ThermoFisher) for cDNA synthesis, followed by qPCR using KAPA SybrFast kit (KAPA Biosystems, KK4601) and the following primers : Forward 5'-TTCCGACGTGCTCGAACTTT-3'; Reverse 5'-CCAACACGGTTGTGACAGTGA-3'. The RT-qPCR assays were performed in duplicates of three independent experiments. For PFU assays, supernatants were used to infect MRC5 cells for 2 h. Cells were then overlaid with culture media containing agarose (1%). After a 48-h incubation, plaque forming units were counted under a light microscope using MTT staining of the cells. The PFU assays were performed in triplicates of a single experiment.

Vero E6 cells were treated with compounds at time of infection by SARS-CoV-2-mNG at MOI=0.01 in DMEM supplemented with 2% FCS. The viral inoculum was removed after a 2-h incubation and the cells were overlaid with fresh DMEM media supplemented with 10% FCS containing the diluted compounds. After a 48-h incubation at 37 °C, supernatants were collected and frozen at – 80 °C prior to quantification and titration by

RT-qPCR and endpoint dilution assay (TCID<sub>50</sub>/mL). RT-qPCR were performed on the collected supernatants. RNA was extracted from supernatant using RNA extraction kit QiAmp viral RNA kit (Qiagen ID 52906). RTqPCR was performed using TaqMan Fast Virus 1-Step MasterMix (ThermoFisher 4444432) and published SARS-CoV2 probes<sup>50</sup>: Forward (IDT 10006888); Reverse (IDT 10006890) Probe (IDT 10006892). Three independent replication assays were performed in triplicates for these viral replication assays. Classic tissue culture infectious dose 50% (TCID<sub>50</sub>/mL) in Vero E6 cells were performed in triplicates on viral stocks and on collected samples using the Reed & Muench statistical method.

**Cytotoxicity assays.** MRC5 cells were treated with compounds for 48 h and MTT assay was performed as reported previously<sup>21</sup>. Cells were incubated with MTT reagent (1.2 mM, Life Technologies, Eugene, OR, USA) for 2 h. Acidic isopropanol was used to dissolve the formazan crystals and cell viability was measured by a spectrophotometer (Bio-Rad, Hercules, CA, USA). WST-1 viability assay was performed on Vero E6 cells treated for 48 h with compounds, following the manufacturer's instructions (Roche Diagnostics GmbH, Mannheim, Germany). The cytotoxicity assays were performed in triplicates.

**Effective concentrations, cytotoxic concentrations and selectivity index calculations.** The 50% effective concentrations (EC<sub>50</sub>), defined as a compound's concentration inhibiting viral replication by 50%, was determined using a four- or three-parameter logistic regression (AAT Bioquest IC<sub>50</sub> Calculator) to fit the dose–response curves. The cytotoxic concentration 50 (CC<sub>50</sub>), defined as a compound's concentration reducing cell viability by 50%, was determined for each compound and cell type by the same method (AAT Bioquest IC<sub>50</sub> Calculator). When our measurements did not reach 50% toxicity or 50% inhibition by studied concentrations, we used the estimated EC<sub>50</sub> or CC<sub>50</sub> value for further calculation of Selectivity Index (indicated as > 200 in Tables 2, 3). The Selectivity Index (SI) was calculated as previously reported<sup>21</sup> by dividing the CC<sub>50</sub> by the EC<sub>50</sub> of every compound for each virus tested. A low SI (< 1) indicates a poor candidate for further development in therapeutic antiviral strategies. A high selectivity index (SI > 1) reflects an important range of concentrations that show an effective antiviral effect with low toxicity.

**Statistical analysis.** RTqPCR experiments were performed in replicates as indicated. Values are presented as means of these independent experiments. Statistical significance or *p* value < 0.05 (represented by \*) was assessed by performing the Wilcoxon signed-rank (value of 100). *P* value < 0.01 (\*\*) or *p* value < 0.001 (\*\*\*) were also represented. This analysis was performed using Graph Pad Prism 6 software.

## Results

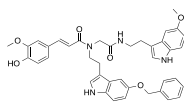
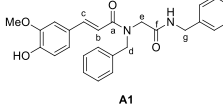
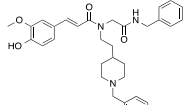
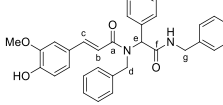
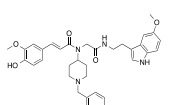
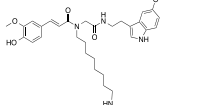
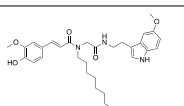
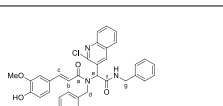
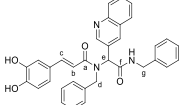
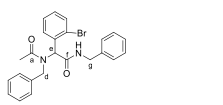
The ten small molecules tested were synthesized at the University of Franche-Comté (Table 1), and were initially assessed as potential treatment for the oxidative stress associated with Alzheimer's disease<sup>44–47</sup>. These molecules were selected based on their structure similarities with already reported inhibitors of nsp5 protease of SARS-CoV-2<sup>42</sup>. Interestingly these compounds have chemical structures close to ferulic acid derivatives (FADs), caffeic acid derivatives (CAFDs) and carboxamide derivatives (CAMDs) (Table 1)<sup>44–47</sup>. Among the ten compounds, eight were FADs, namely LIJ2P40, OS4-1, MBA108-1, MBA33, MBA152, 5c, MBA112 and MBA28. MBA27-1 is a CAFD and MBA140 is a CAMD.

Among these ten small molecules tested, five, MBA112, MBA33, MBA27-1, OS4-1 and MBA108-1, showed high cytotoxicity on MRC5 cells with a CC<sub>50</sub> of 35.5 μM, 39.4 μM, 22.5 μM, 8.0 μM and 34.4 μM respectively (Fig. 1A, Table 2). In addition, two molecules MBA152 and 5c displayed moderate cytotoxicity with a CC<sub>50</sub> of 108.3 μM and 89.0 μM respectively (Fig. 1B, Table 2). By contrast, three molecules MBA140, LIJ2P40, and MBA28 showed low cytotoxicity on MRC5 cells with a CC<sub>50</sub> above 200 μM (Fig. 1C, Table 2), and were further tested.

The three less cytopathic drugs (MBA28, MBA140 and LIJ2P40) were tested for their ability to inhibit viral replication of HCoV-229E in MRC5 cells. Cells were infected by HCoV-229E MOI = 1 during two hours in presence of various concentrations of each drug (0.1, 5, 10, 50, 100 or 200 μM). After infection, cells were cultured in presence of treatment or not and viral replication was analyzed in supernatant after 48 h either by RT-qPCR (Fig. 2A) or Plaque Forming Unit assay (PFU) (Fig. 2B). Taken together, our data suggest a decreasing viral replication, measured by RT-qPCR, with all three drugs (Fig. 2A). We were also able to observe only a moderate inhibition of replication of HCoV-229E by PFU assays at higher concentrations (> 50 μM) (Fig. 2B).

Based on the preliminary results obtained using the HCoV-229E model, we also tested the ability of MBA28, MBA140 and LIJ2P40 to inhibit viral replication of SARS-CoV-2-mNG in VeroE6 cells. First, the cytotoxicity of LIJ2P40, MBA140 and MBA28 on Vero E6 cells was tested by WST-1 (Fig. 3). Results showed that below 50 μM, all three drugs MBA28, MBA140 and LIJ2P40 showed a moderate toxicity, with a CC<sub>50</sub> above 200 μM for MBA28, a CC<sub>50</sub> of 174.3 μM for MBA140 and a CC<sub>50</sub> of 192.6 μM for LIJ2P40 (Table 3). Higher concentrations (200 μM) showed a moderate effect on VeroE6 cells for MBA28 and more important toxicity for MBA140 and LIJ2P40.

The moderate toxicity of tested compounds further encouraged us to test their antiviral properties of SARS-CoV2-mNG by performing infections at MOI = 0.01 during two hours on VeroE6 cells in presence of treatment or not. Cells were then cultured during 48 h in presence of various concentrations of each drug (0, 1, 5, 10, 50, 100 or 200 μM), and viral replication was analyzed in supernatant either by RT-qPCT (Fig. 4A) or endpoint dilution assays (TCID<sub>50</sub>) (Fig. 4B). We observed a significant decrease in SARS-CoV-2-mNG replication under MBA28 treatment at concentrations of and above 100 μM, with a 46% maximal inhibition at 200 μM (Fig. 4A). For MBA140 treatment, we observed a similar significant decrease in SARS-CoV-2-mNG replication at concentrations starting at 100 μM, with a 58% maximal inhibition (Fig. 4A). By contrast, the maximal percentage

FAD		FAD	
Structure	Name	Structure	Name
 Chemical Formula: C <sub>22</sub> H <sub>26</sub> N <sub>2</sub> O <sub>4</sub> Molecular Weight: 412.76200	LIJ2P40	 A1 C <sub>22</sub> H <sub>26</sub> N <sub>2</sub> O <sub>4</sub> MW: 430.50 g.mol <sup>-1</sup>	OS4-1
 Chemical Formula: C <sub>23</sub> H <sub>29</sub> N <sub>2</sub> O <sub>4</sub> Molecular Weight: 441.69200	MBA 108-1	 A2 C <sub>22</sub> H <sub>26</sub> N <sub>2</sub> O <sub>4</sub> MW: 506.59 g.mol <sup>-1</sup>	MBA 33
 Chemical Formula: C <sub>23</sub> H <sub>29</sub> N <sub>2</sub> O <sub>4</sub> Molecular Weight: 598.72800	MBA 152	 Chemical Formula: C <sub>24</sub> H <sub>29</sub> N <sub>2</sub> O <sub>4</sub> Molecular Weight: 731.98800	MBA112
 Chemical Formula: C <sub>24</sub> H <sub>29</sub> N <sub>2</sub> O <sub>4</sub> Molecular Weight: 747.95700	5c	 A8 C <sub>25</sub> H <sub>30</sub> ClN <sub>2</sub> O <sub>4</sub> MW: 992.08 g.mol <sup>-1</sup>	MBA28
CAFD		CAMD	
Structure	Name	Structure	Name
 A8 C <sub>24</sub> H <sub>29</sub> N <sub>2</sub> O <sub>4</sub> MW: 543.61 g.mol <sup>-1</sup>	MBA27-1	 A13 C <sub>24</sub> H <sub>29</sub> BrN <sub>2</sub> O <sub>2</sub> MW: 451.36 g.mol <sup>-1</sup>	MBA140

**Table 1.** The ten small-molecules tested belonging to the FADs, the CAFDs or the CAMDs.

of inhibition of SARS-CoV-2-mNG reached 82% with an LIJ2P40 concentration of 200  $\mu$ M. We also observed a significant decrease in SARS-CoV-2-mNG replication starting at 50  $\mu$ M of LIJ2P40, with a 42% decrease of viral replication measured by RT-qPCR (Fig. 4A). The inhibition of SARS-CoV-2-mNG replication observed in cells treated with LIJ2P40 did not follow the reduction in cell viability and was a genuine anti-SARS-CoV-2 effect of this drug in vitro.

Inhibition of SARS-CoV2-mNG replication was also observed by TCID50 assay at concentrations > 100  $\mu$ M for MBA28 and LIJ2P40 (Fig. 4B). Overall, among the three drugs tested, LIJ2P40 showed the highest anti-SARS-CoV-2 activity.

Based on these results, we measured an EC<sub>50</sub> above 200  $\mu$ M for MBA28, of 176.3  $\mu$ M for MBA140 and LIJ2P40 showed the lowest EC<sub>50</sub> at 66.5  $\mu$ M (Table 3). We calculated the selectivity index for the inhibition of SARS-CoV-2-mNG in Vero E6 cells for the three drugs tested. Both MBA28 and MBA140 present a low SI, both below or equal to 1 (Table 3). The SI for LIJ2P40 is higher, above 2.9 (Table 3) showing an interesting potential for further testing in other models and potentially therapeutic antiviral strategies against coronaviruses infections.

## Discussion

We showed the antiviral effect of ferulic acid derivatives, notably MBA28, MBA140 and LIJ2P40, on HCoV-229E and SARS-CoV-2 replication in vitro. These drugs showed a decrease in HCoV-229E replication, as measured by RT-qPCR. However, the important variation between biological replicates did not allow us to conclude based on these data. The SD values obtained were still very important due to difficulties in the technical replication of the experiments. As the experimental conditions were not entirely optimized and the sensitivity of the assay was not as good as it should be, we decided not to conclude on these data. In addition, the assessment of the compounds effect on HCoV-229E replication is an intermediate step in our testing pipeline, where SARS-CoV-2 inhibition is our main focus.

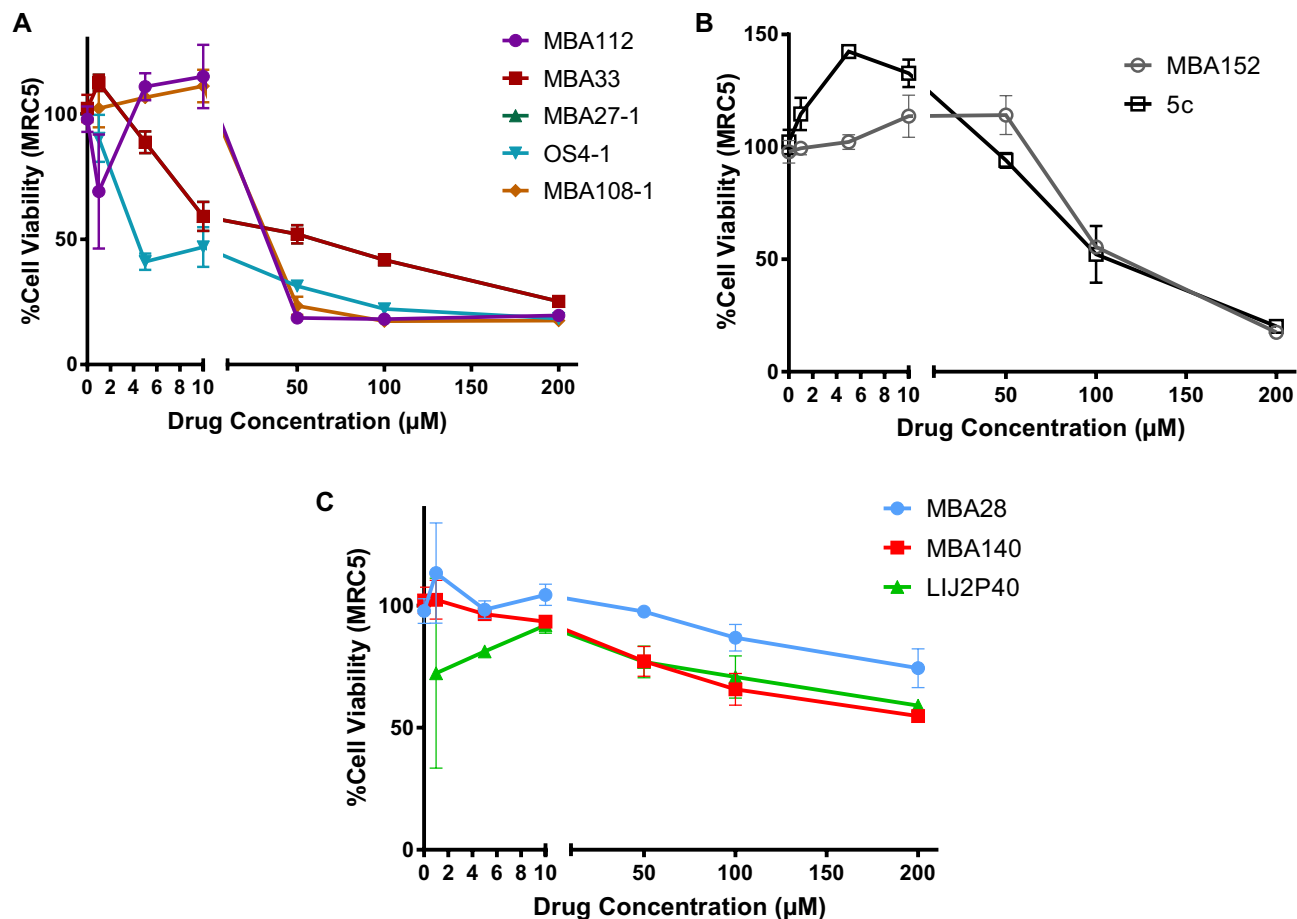


**Figure 1.** Viability of MRC5 cells under treatment with the ten drugs using MTT toxicity assay. (A) High cytotoxicity was observed for MBA112, MBA33, MBA27-1, OS4-1 and MBA108-1, (B) intermediate cytotoxicity for MBA152 and 5c and (C) low cytotoxicity for MBA140, LIJ2P40, and MBA28. MTT assays were performed after 48 h. Untreated cells were used for normalization of MTT assay. Results are represented as mean  $\pm$  SD of three independent experiments.

Drug tested	CC50 ( $\mu$ M)
MBA112	35.5
MBA33	39.4
MBA27-1	22.5
OS4-1	8.0
MBA108-1	34.4
MBA 152	108.3
5c	89.0
MBA28	> 200
MBA140	> 200
LIJ2P40	> 200

**Table 2.** CC50 on MRC5 cells of the ten drugs studied for their toxicity.

The overall efficiency of these three drugs against HcoV-229E is too limited to warrant their use as is, but they could be good candidates as base molecules to be modified for enhanced antiviral effect. We however considered them having enough potential to be further tested on SARS-CoV-2.

We observed a moderate cytotoxicity of MBA28 on Vero E6 cells, with a CC50 of > 200  $\mu$ M and 174.3  $\mu$ M for MBA140. The testing of LIJ2P40 however showed a more gentle cytotoxicity at lower concentrations, however high concentration of 200  $\mu$ M showed important toxicity. Indeed the effect of the solvent used to solubilize the compounds (DMSO) are expected to impact the viability assays results, especially at high concentrations (2%).

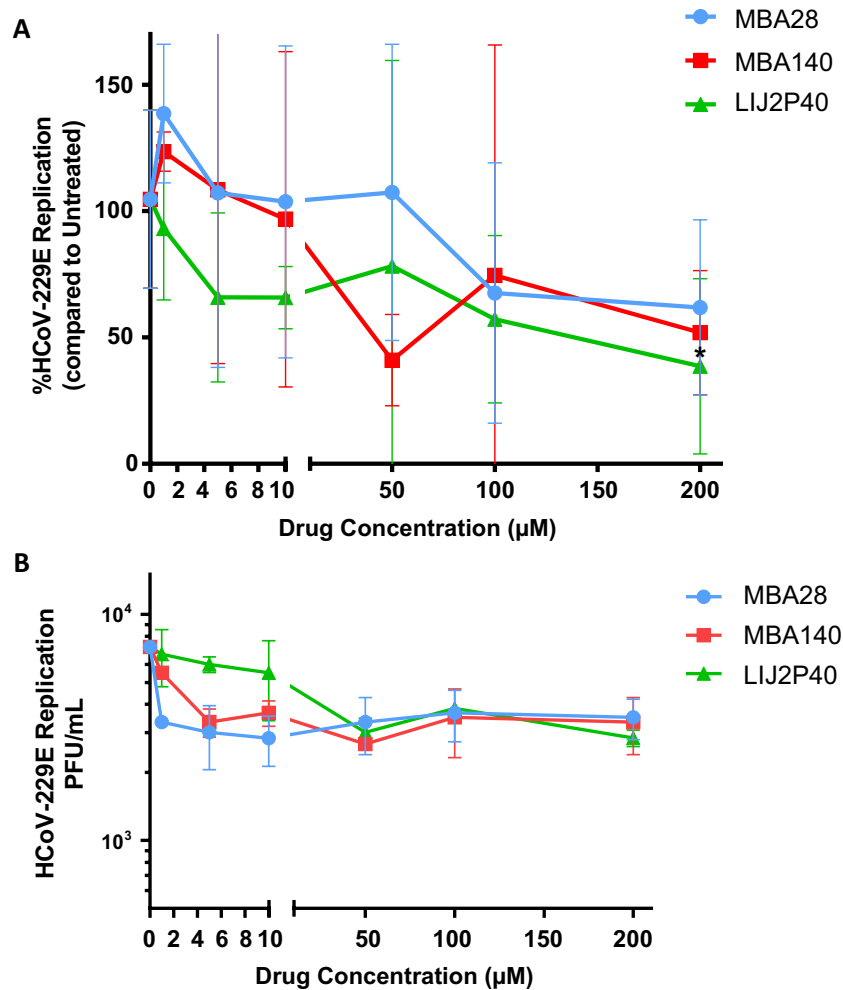


**Figure 2.** Inhibition of replication of high HCoV-229E viral load measured by RT-qPCR (A) and PFU assay (B) on MRC5 cells by LIJ2P40, MBA140 and MBA28. Cells were treated by compounds at the time of infection with HCoV-229E (MOI = 1). PFU assay and RT-qPCR were performed after 48 h. Untreated cells infected with HCoV-229E ( $864.10^4$  copies/mL) were used for normalization. RT-qPCR results are represented as mean  $\pm$  SD of three independent experiments done in duplicates. PFU assay results are represented as mean  $\pm$  SD of a single experiment done in triplicates. The Wilcoxon signed-rank test (value of 100) was used as statistical test with  $P \leq 0.05 = *$ .

Additional testing of possible solvents and their effects should be performed and taken into account for pursuing more advanced antiviral testing. Also, a small increase in viability at the highest concentration (200  $\mu$ M) was globally observed for MBA28, compared to 100  $\mu$ M. This could be the results of the antioxidant properties of the molecule<sup>36</sup>. Since the viability was measured using WST-1 assay, an antioxidant could impact the tetrazolium reduction, which is measured by such assay<sup>51</sup>. This effect might be more pronounced at higher concentrations.

The moderate cytotoxicity measured in Vero E6 cells warranted the further testing of these three drugs for SARS-CoV-2 inhibition. We observed a decrease in SARS-CoV-2-mNG replication in vitro at high doses of MBA28 ( $EC_{50} > 200$   $\mu$ M) and at high doses of MBA140 ( $EC_{50} = 176.3$   $\mu$ M). As we did note the TCID<sub>50</sub> assay showed an increase in SARS-CoV-2-mNG replication at 200  $\mu$ M dose of MBA140, compared to 100  $\mu$ M, we do need to underline the limited number of replicates in these experiments. However, our RT-qPCR results, which is a more sensitive and reproducible method, and also based on triplicates of three independent experiments, showed a significant inhibition at those concentrations thereby providing strong evidence toward the antiviral effect observed. In addition, we found a significant inhibition of SARS-CoV-2-mNG replication with LIJ2P40, starting at 50  $\mu$ M concentration ( $EC_{50} = 66.5$   $\mu$ M). Regarding LIJ2P40 treatment, TCID results, however poor in replicates, did show an interesting decrease of two logs at higher concentrations. While the toxicity at these concentrations was notable, the significant reduction of mean replication compared to untreated as measured by RT-qPCR showed an additional inhibition by 18%, demonstrating a genuine antiviral effect for this molecule. Therefore, of the three drugs tested against SARS-CoV-2-mNG, LIJ2P40 showed the most promising inhibition of SARS-CoV-2 replication, with limited toxicity. To further confirm the anti-SARS-CoV-2 effect of these drug using an in vitro model closer to the in vivo pathophysiology, we will assess their effect on SARS-CoV-2-mNG infections using human respiratory tract epithelial cell lines, for instance lung epithelial cell lines A549 and Calu

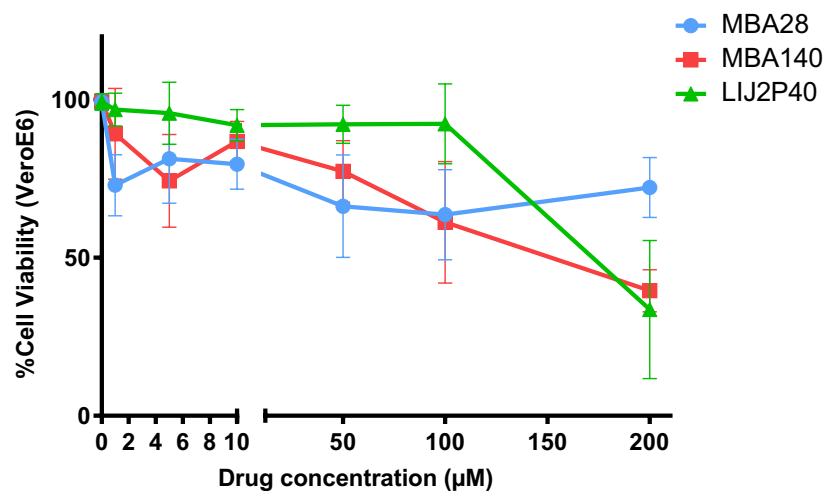


**Figure 3.** Viability of Vero E6 cells treated with MBA28, MBA140 or LIJ2P40 drugs measured by WST-1 assay. WST-1 viability assays were performed after 48 h. Untreated cells were used for normalization of the WST-1 viability assay. Results are represented as mean  $\pm$  SD of three biological replicates.

Drug tested	CC50 ( $\mu$ M)	EC50 ( $\mu$ M)	SI
MBA 28	> 200	> 200	< 1
MBA 140	174.3	176.3	1
LIJ2P40	192.6	66.5	2.9

**Table 3.** EC50, CC50 and SI for the 3 drugs tested for SARS-CoV-2 replication in VeroE6 cells.

or nasal epithelial cell line RPMI2650. Additionally, 3D organotypic nasal epithelial cultures (commercially available MucilAir™) could be used to better reflecting the pathophysiology of SARS-CoV-2 infection than the current macaque renal epithelial model of Vero E6 cells.

Polyphenols have been previously showed to be efficient against viral infections, by acting on the modulation of immune system<sup>52</sup>. They were also shown to directly inhibit viral replication<sup>53</sup> or reduce viral entry<sup>54</sup>. CAFDs are phenolic compounds which possess prominent antiviral activity especially against hepatitis B virus (HBV) and HIV<sup>55</sup>. Recent docking analysis on CAFDs showed that they possessed high binding energies against the main protease Nsp5 ( $M^{pro}$ ), Nsp15 and the S2 spike subunit of SARS-CoV-2. They could be potent modulators of Covid-19, since their binding energy is even higher than nelfinavir<sup>19</sup>.

FADs, as part of phenols, share properties with other polyphenols such as resveratrol. The observed antiviral effects could be linked to their interactions with both viral proteases (Nsp3 and Nsp5) but also with the spike protein. The phenol groups could allow the disruption of the enzymatic function of Nsp3 and Nsp5. The interaction with spike proteins could also prevent capsid formation, thus reducing the viral replication.

A similarity of FADs and CAFs chemical structure with previously reported small molecules<sup>42</sup> could explain their potential as antiviral drugs. These small molecules were predicted to target  $M^{pro}$  of SARS- and MERS-CoV, by the presence of hydrophobic regions. The disruption of  $M^{pro}$  protease activity results in an important inhibition of viral replication<sup>56</sup>. CAMDs have been reported to display antiviral activity against RNA viruses including influenza virus, parainfluenza virus, norovirus, SARS-CoV and SARS-CoV-2<sup>37–41</sup>. Therefore we tested the anti-coronavirus activity of MBA140, a carboxamide derivative newly synthesized, which displays the closest chemical structure to an oxazole-carboxamide derivative previously reported as efficient against SARS-CoV<sup>41</sup>. Although MBA140 inhibits both HCoV-229E and SARS-CoV2 its antiviral effect was limited and precludes its further testing in preclinical models of SARS-CoV-2.

## Conclusions

The overall efficiency of the FAD compounds MBA28 and the CAMD compound MBA140 against SARS-CoV-2 is too limited to warrant their use as is, but they could be good candidates as base molecules to be modified for enhanced antiviral effect in the future. In addition, we show here the antiviral effect of the FAD LIJ2P40, both on HCoV-229E and SARS-CoV-2 replication in vitro. Our testing for SARS-CoV-2 inhibition shows a strong antiviral effect of LIJ2P40 with moderate cytotoxicity in vitro. However, further testing in more physiological in vitro models of human respiratory tract epithelial cell lines and 3D organotypic nasal epithelial (MucilAir™) cultures is needed to confirm whether these compounds could be of use in a clinical setting, alone or in combination with other treatments. Finally, it is important to note that our results on SARS-CoV-2 inhibition are in vitro data and

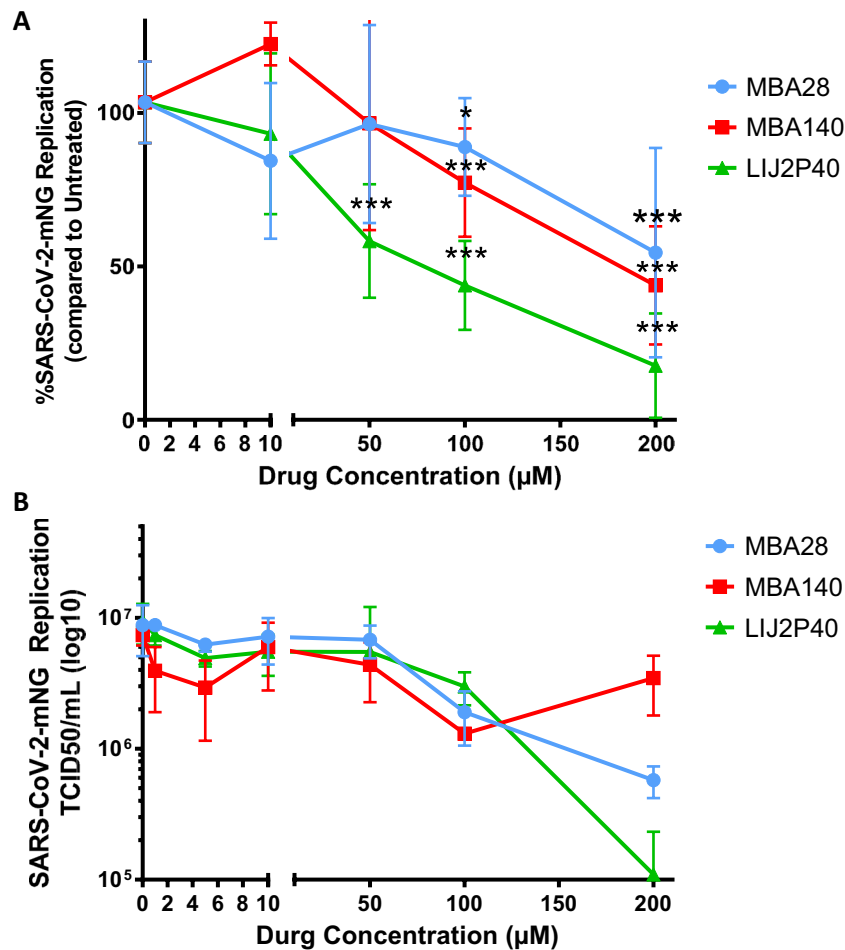


**Figure 4.** Inhibition of SARS-CoV-2-mNG replication in VeroE6 cells measured by RT-qPCR (A) and endpoint dilution (TCID50/mL) (B), for LIJ2P40, MBA140 and MBA28. Cells were treated by compounds at the time of infection with SARS-CoV2-mNG (MOI=0.01). Endpoint dilution assays and RT-qPCR were performed 48 h post-infection. Untreated cells infected with SARS-CoV2-mNG (527.10<sup>6</sup> copies/mL) were used for normalization of the assay. RT-qPCR results are represented as mean  $\pm$  SD of three independent experiments done in triplicates. TCID50 results are represented as mean  $\pm$  SD of a single experiment done in triplicates. The Wilcoxon signed-rank test (value of 100) was used as statistical test with  $P \leq 0.05 = *$ ;  $P \leq 0.01 = **$ ;  $P \leq 0.001 = ***$ .

do not indicate that any of the drugs tested can be used to treat Covid-19 until double-blinded clinical assays have been successfully performed.

### Data availability

The datasets used and/or analyzed during the current study are available from the corresponding author on reasonable request.

Received: 1 December 2021; Accepted: 18 November 2022

Published online: 24 November 2022

### References

- Phan, M. V. T. *et al.* Identification and characterization of Coronaviridae genomes from Vietnamese bats and rats based on conserved protein domains. *Virus Evol.* **4**, vey035 (2018).
- Lim, Y. X., Ng, Y. L., Tam, J. P. & Liu, D. X. Human coronaviruses: A review of virus-host interactions. *Diseases* **4**, 26 (2016).
- Chan, J.F.-W. *et al.* Genomic characterization of the 2019 novel human-pathogenic coronavirus isolated from a patient with atypical pneumonia after visiting Wuhan. *Emerg. Microbes Infect.* **9**, 221–236 (2020).
- van der Hoek, L. Human coronaviruses: What do they cause?. *Antivir. Ther. (Lond.)* **12**, 651–658 (2007).
- Fehr, A. R. & Perlman, S. Coronaviruses: An overview of their replication and pathogenesis. *Methods Mol. Biol.* **1282**, 1–23 (2015).
- Zheng, J. SARS-CoV-2: An Emerging Coronavirus that Causes a Global Threat. *Int. J. Biol. Sci.* **16**, 1678–1685 (2020).
- Geng, Y.-J. *et al.* Pathophysiological characteristics and therapeutic approaches for pulmonary injury and cardiovascular complications of coronavirus disease 2019. *Cardiovasc. Pathol.* <https://doi.org/10.1016/j.carpath.2020.107228> (2020).
- Krammer, F. SARS-CoV-2 vaccines in development. *Nature* **586**, 516–527 (2020).
- Recovery Collaborative Group *et al.* Dexamethasone in Hospitalized Patients with Covid-19. *N. Engl. J. Med.* **384**, 693–704 (2021).



10. Selvaraj, V. *et al.* Tocilizumab in hospitalized patients with COVID-19: A meta analysis of randomized controlled trials. *Lung* **199**, 239–248 (2021).
11. Marconi, V. C. *et al.* Efficacy and safety of baricitinib for the treatment of hospitalised adults with COVID-19 (COV-BARRIER): A randomised, double-blind, parallel-group, placebo-controlled phase 3 trial. *Lancet Respir. Med.* **9**, 1407–1418 (2021).
12. Selvaraj, V. *et al.* Baricitinib in hospitalised patients with COVID-19: A meta-analysis of randomised controlled trials. *eClinicalMedicine* **49**, 101489 (2022).
13. Nappi, F., Iervolino, A. & Avtaar Singh, S. S. Molecular insights of SARS-CoV-2 antivirals administration: A balance between safety profiles and impact on cardiovascular phenotypes. *Biomedicines* **10**, 437 (2022).
14. Sanders, J. M., Monogue, M. L., Jodlowski, T. Z. & Cutrell, J. B. Pharmacologic treatments for coronavirus disease 2019 (COVID-19): A review. *JAMA* <https://doi.org/10.1001/jama.2020.6019> (2020).
15. Chen, W.-H., Strych, U., Hotez, P. J. & Bottazzi, M. E. The SARS-CoV-2 vaccine pipeline: An overview. *Curr. Trop. Med. Rep.* <https://doi.org/10.1007/s40475-020-00201-6> (2020).
16. Zhou, Y. *et al.* Network-based drug repurposing for novel coronavirus 2019-nCoV/SARS-CoV-2. *Cell Discov.* **6**, 1–18 (2020).
17. Pyrc, K., Berkhout, B. & van der Hoek, L. Antiviral strategies against human coronaviruses. *Infect Disord. Drug Targets* **7**, 59–66 (2007).
18. Dos Santos, C. N., Menezes, R. & Stewart, D. Polyphenols as new leads in drug discovery: Biological activity and mechanisms. *Curr. Pharm. Des.* **24**, 2041–2042 (2018).
19. Adem, Ş *et al.* Caffeic acid derivatives (CAFDs) as inhibitors of SARS-CoV-2: CAFDs-based functional foods as a potential alternative approach to combat COVID-19. *Phytomedicine* **85**, 153310 (2021).
20. Salehi, B. *et al.* Resveratrol: A double-edged sword in health benefits. *Biomedicines* **6**, 91 (2018).
21. Pasquereau, S. *et al.* Resveratrol inhibits HCoV-229E and SARS-CoV-2 coronavirus replication in vitro. *Viruses* **13**, 354 (2021).
22. Zhou, Z.-X., Mou, S.-F., Chen, X.-Q., Gong, L.-L. & Ge, W.-S. Anti-inflammatory activity of resveratrol prevents inflammation by inhibiting NF-κB in animal models of acute pharyngitis. *Mol. Med. Rep.* **17**, 1269–1274 (2018).
23. Camins, A. *et al.* Resveratrol: An antiaging drug with potential therapeutic applications in treating diseases. *Pharmaceuticals (Basel)* **2**, 194–205 (2009).
24. Palamara, A. T. *et al.* Inhibition of influenza A virus replication by resveratrol. *J. Infect. Dis.* **191**, 1719–1729 (2005).
25. Mohd, A., Zainal, N., Tan, K.-K. & AbuBakar, S. Resveratrol affects Zika virus replication in vitro. *Sci. Rep.* **9**, 14336 (2019).
26. Mastromarino, P. *et al.* Resveratrol inhibits rhinovirus replication and expression of inflammatory mediators in nasal epithelia. *Antiviral Res.* **123**, 15–21 (2015).
27. Huang, H. *et al.* Antiviral activities of resveratrol against rotavirus in vitro and in vivo. *Phytomedicine* <https://doi.org/10.1016/j.phymed.2020.153230> (2020).
28. Lin, S.-C. *et al.* Effective inhibition of MERS-CoV infection by resveratrol. *BMC Infect. Dis.* **17**, 144 (2017).
29. Cao, S., Realegeno, S., Pant, A., Satheshkumar, P. S. & Yang, Z. Suppression of poxvirus replication by resveratrol. *Front Microbiol.* **8**, 2196 (2017).
30. Berardi, V., Ricci, F., Castelli, M., Galati, G. & Risuleo, G. Resveratrol exhibits a strong cytotoxic activity in cultured cells and has an antiviral action against polyomavirus: Potential clinical use. *J. Exp. Clin. Cancer Res.* **28**, 96 (2009).
31. Chávez, J. H. *et al.* Evaluation of antiviral activity of phenolic compounds and derivatives against rabies virus. *Vet. Microbiol.* **116**, 53–59 (2006).
32. Hariono, M. *et al.* Potential new H1N1 neuraminidase inhibitors from Ferulic acid and vanillin: Molecular modelling, synthesis and in vitro assay. *Sci. Rep.* **6**, 38692 (2016).
33. Langland, J., Jacobs, B., Wagner, C. E., Ruiz, G. & Cahill, T. M. Antiviral activity of metal chelates of caffeic acid and similar compounds towards herpes simplex, VSV-Ebola pseudotyped and vaccinia viruses. *Antiviral Res.* **160**, 143–150 (2018).
34. Ogawa, M. *et al.* Caffeic acid, a coffee-related organic acid, inhibits infection by severe fever with thrombocytopenia syndrome virus in vitro. *J. Infect. Chemother.* **24**, 597–601 (2018).
35. Utsunomiya, H. *et al.* Inhibition by caffeic acid of the influenza A virus multiplication in vitro. *Int. J. Mol. Med.* **34**, 1020–1024 (2014).
36. Alam, M. A. Anti-hypertensive effect of cereal antioxidant ferulic acid and its mechanism of action. *Front. Nutr.* **6**, 121 (2019).
37. Ohba, M. *et al.* Discovery and synthesis of heterocyclic carboxamide derivatives as potent anti-norovirus agents. *Chem. Pharm. Bull. (Tokyo)* **64**, 465–475 (2016).
38. Fedorova, V. A. *et al.* Antiviral activity of amides and carboxamides of quinolizidine alkaloid (-)-cytisine against human influenza virus A (H1N1) and parainfluenza virus type 3. *Nat. Prod. Res.* <https://doi.org/10.1080/14786419.2019.1696791> (2019).
39. Cheng, H. *et al.* Design, synthesis, and in vitro biological evaluation of 1H-1,2,3-triazole-4-carboxamide derivatives as new anti-influenza A agents targeting virus nucleoprotein. *J. Med. Chem.* **55**, 2144–2153 (2012).
40. Beylkin, D. *et al.* Protein-structure assisted optimization of 4,5-dihydroxypyrimidine-6-carboxamide inhibitors of influenza virus endonuclease. *Sci. Rep.* **7**, 17139 (2017).
41. Adedeji, A. O. *et al.* Novel inhibitors of severe acute respiratory syndrome coronavirus entry that act by three distinct mechanisms. *J. Virol.* **87**, 8017–8028 (2013).
42. Morse, J. S., Lalonde, T., Xu, S. & Liu, W. R. Learning from the past: Possible urgent prevention and treatment options for severe acute respiratory infections caused by 2019-nCoV. *ChemBioChem* **21**, 730–738 (2020).
43. Xie, X. *et al.* An infectious cDNA clone of SARS-CoV-2. *Cell Host Microbe* **27**, 841–848.e3 (2020).
44. Benckekroun, M. *et al.* The antioxidant additive approach for Alzheimer's disease therapy: New ferulic (Lipoic) acid plus melatonin modified tacrines as cholinesterases inhibitors, direct antioxidants, and nuclear factor (erythroid-derived 2)-like 2 activators. *J. Med. Chem.* **59**, 9967–9973 (2016).
45. Benckekroun, M. *et al.* Donepezil-ferulic acid hybrids as anti-Alzheimer drugs. *Fut. Med. Chem.* **7**, 15–21 (2015).
46. Benckekroun, M. *et al.* Synthesis, antioxidant and Aβ anti-aggregation properties of new ferulic, caffeic and lipoic acid derivatives obtained by the Ugi four-component reaction. *Bioorg. Chem.* **85**, 221–228 (2019).
47. Pachón-Angona, I. *et al.* Synthesis of new ferulic/lipoic/comenic acid-melatonin hybrids as antioxidants and Nrf2 activators via Ugi reaction. *Fut. Med. Chem.* **11**, 3097–3108 (2019).
48. Baer, A. & Kehn-Hall, K. Viral concentration determination through plaque assays: Using traditional and novel overlay systems. *J. Vis. Exp.* <https://doi.org/10.3791/52065> (2014).
49. Vijgen, L. *et al.* Development of one-step, real-time, quantitative reverse transcriptase PCR assays for absolute quantitation of human coronaviruses OC43 and 229E. *J. Clin. Microbiol.* **43**, 5452–5456 (2005).
50. Corman, V. M. *et al.* Detection of 2019 novel coronavirus (2019-nCoV) by real-time RT-PCR. *Eurosurveillance* **25**, 2000045 (2020).
51. Scarcello, E., Lambremont, A., Vanbever, R., Jacques, P. J. & Lison, D. Mind your assays: Misleading cytotoxicity with the WST-1 assay in the presence of manganese. *PLoS ONE* **15**, e0231634 (2020).
52. Jasso-Miranda, C. *et al.* Antiviral and immunomodulatory effects of polyphenols on macrophages infected with dengue virus serotypes 2 and 3 enhanced or not with antibodies. *Infect Drug Resist* **12**, 1833–1852 (2019).
53. Lalani, S. & Poh, C. L. Flavonoids as Antiviral agents for enterovirus A71 (EV-A71). *Viruses* **12**, 184 (2020).
54. Vázquez-Calvo, Á., Jiménez de Oya, N., Martín-Acebes, M. A., Garcia-Moruno, E. & Saiz, J.-C. Antiviral properties of the natural polyphenols Delphinidin and epigallocatechin Gallate against the Flaviviruses west Nile virus, Zika virus, and dengue virus. *Front Microbiol.* **8**, 1314 (2017).

55. Pluymsers, W. *et al.* Inhibition of human immunodeficiency virus type 1 integration by diketo derivatives. *Antimicrob. Agents Chemother.* **46**, 3292–3297 (2002).
56. Qiao, J. *et al.* SARS-CoV-2 Mpro inhibitors with antiviral activity in a transgenic mouse model. *Science* **371**, 1374–1378 (2021).

### Author contributions

Conceptualization, G.H.; formal analysis, S.P., M.G., M.B., I.P.A.; investigation, S.P., M.G., M.B., I.P.A., L.I. and S.M.B.; writing—original draft preparation, S.P., M.G., C.V.L., L.I. and G.H.; writing—review and editing, S.P., M.G., M.B., L.I., S.M.B., C.V.L. and G.H.; visualization, S.P.; supervision, C.V.L., L.I., G.H.; project administration, G.H.; funding acquisition, C.V.L., L.I., G.H. All authors have read and agreed to the published version of the manuscript.

### Funding

This research was funded by University of Franche-Comté, the University of Bourgogne-Franche-Comté, and the Région Bourgogne-Franche-Comté (2021-Y-08292 and 2021-Y-08290) (to G.H.). This work was supported by the Regional Council of Franche-Comté (2016YC-04540 and 04560) (to L.I.). C.V.L. acknowledges funding from the Belgian National Fund for Scientific Research (FRS-FNRS, Belgium), Les Amis des Instituts Pasteur à Bruxelles and the Université Libre de Bruxelles (ULB). The laboratory of CVL is part of the ULB-Cancer Research Centre (U-CRC). MG is funded by a fellowship IF@ULB program from “European Union’s Horizon 2020 research and innovation programme under the Marie Skłodowska-Curie Grant Agreement No 801505”. MB is a fellow of the “FRRIA Program” (F.R.S-FNRS). CVL is “Directeur de Recherches” of the F.R.S-FNRS.

### Competing interests

The authors declare no competing interests.

### Additional information

**Correspondence** and requests for materials should be addressed to G.H.

**Reprints and permissions information** is available at [www.nature.com/reprints](http://www.nature.com/reprints).

**Publisher’s note** Springer Nature remains neutral with regard to jurisdictional claims in published maps and institutional affiliations.



**Open Access** This article is licensed under a Creative Commons Attribution 4.0 International License, which permits use, sharing, adaptation, distribution and reproduction in any medium or format, as long as you give appropriate credit to the original author(s) and the source, provide a link to the Creative Commons licence, and indicate if changes were made. The images or other third party material in this article are included in the article’s Creative Commons licence, unless indicated otherwise in a credit line to the material. If material is not included in the article’s Creative Commons licence and your intended use is not permitted by statutory regulation or exceeds the permitted use, you will need to obtain permission directly from the copyright holder. To view a copy of this licence, visit <http://creativecommons.org/licenses/by/4.0/>.

© The Author(s) 2022